

Extreme MetaboHealth scores in three cohort studies associate with plasma protein markers for inflammation and cholesterol transport.

D. Bizzarri^{1,2,3}, E.B. van den Akker^{1,2,3}, M.J.T. Reinders^{2,3}, R. Pool^{4,5}, M. Beekman¹, N. Lakenberg¹, N. Drouin^{6,7,8}, K.E. Stecker^{7,8}, A.J.R. Heck^{7,8}, E.F. Knol⁹, J.M. Vergeer¹⁰, M.A. Ikram¹⁰, M. Ghanbari¹⁰, A.J. van Gool¹¹, BBMRI-NL¹², D.I. Boomsma^{4,5,13,14}, and P.E. Slagboom^{1,14#}

¹ Department of Biomedical Data Sciences, Molecular Epidemiology, LUMC, Leiden, The Netherlands

² Department of Biomedical Data Sciences, Leiden Computational Biology Center, LUMC, Leiden, The Netherlands

³ Delft Bioinformatics Lab, Delft University of Technology, Delft, The Netherlands

⁴ Department of Biological Psychology, Vrije Universiteit Amsterdam, Amsterdam, The Netherlands.

⁵ Amsterdam Public Health Research Institute, Amsterdam, The Netherlands

⁶ Leiden Academic Centre for Drug Research, Leiden University, Leiden, Netherlands

⁷ Biomolecular Mass Spectrometry and Proteomics, Bijvoet Center for Biomolecular Research and Utrecht Institute for Pharmaceutical Sciences, Utrecht University, Utrecht, The Netherlands

⁸ Netherlands Proteomics Center, Utrecht, The Netherlands

⁹ Center of Translational Immunology and Dermatology/Allergology, University Medical Center Utrecht, Utrecht, The Netherlands

¹⁰ Department of Epidemiology, Erasmus MC, Rotterdam, the Netherlands

¹¹ Translational Metabolic Laboratory, Department of Laboratory Medicine, Radboud University

Medical Center, Nijmegen, the Netherlands

¹² BBMRI-NL: <https://www.bbMRI.nl>; see Consortium Banner Supplement S1

¹³ Amsterdam Reproduction and Development (AR&D) Research Institute, Amsterdam, The Netherlands.

¹⁴ Dept of Complex Trait Genetics, Center for Neurogenomics and Cognitive Research, Amsterdam, Vrije Universiteit Amsterdam

¹⁵ Max Planck Institute for the Biology of Ageing, Cologne, Germany

33 **ABSTRACT**

34 The MetaboHealth score is a highly informative health indicator in ageing studies and yet
35 contains only a small number of metabolites. Here we estimate the heritability of the score
36 in 726 monozygotic (MZ) and 450 dizygotic (DZ) twin pairs, and test for association with
37 plasma proteins by comparing extreme scoring individuals selected from two large
38 population cohorts -the Leiden Longevity Study (LLS) and the Rotterdam Study (RS) and
39 discordant monozygotic twin pairs from the Netherlands Twin Register (NTR).

40 The heritability for the MetaboHealth score was estimated at 40%. In 50 high and 50 low
41 scoring MetaboHealth groups from LLS and RS, we uncovered significant differences in
42 plasma proteins, notably in 3 (out of 15) cytokines (GDF15, IL6, and MIG), and 106 proteins
43 (out of 289) as determined by Mass Spectrometry based proteomics analysis. A high
44 MetaboHealth score associated with an increased level for 42 serum proteins,
45 predominantly linked to inflammation and immune response, including CRP and HPT. A low
46 score associated with decreased levels of 71 proteins enriched in high-density lipoprotein
47 (HDL) remodeling and cholesterol transport pathways, featuring proteins such as APOA1,
48 APOA2, APOA4, and TETN.

49 In MZ twins selected for maximal discordance within a pair we found 68 serum proteins
50 associated with the MetaboHealth score indicating that a minor part of the associations
51 observed in LLS and RS is likely explained by genetic influences. Taken together, our study
52 sheds light on the intricate interplay between MetaboHealth, plasma proteins, cytokines,
53 and genetic influences, paving the way for future investigations aimed at optimizing this
54 mortality risk indicator.

55 INTRODUCTION

56 As the global human population rapidly ages, it is valuable to measure vulnerability and
57 expected resilience of older individuals to support prevention and well-informed treatment
58 aimed at enhancing well-being [1]. Efficient disease prevention hinges on possibilities for
59 evaluating not only an individual's disease risk, but also the overall physiological vulnerability
60 in an early stage which is often referred to as biological age. Originally the biological age of
61 individuals was estimated from a suite of physiological tests and biochemical clinical
62 quantifications [2]. More recently explorations shifted towards comprehensive molecular
63 ('omics') datasets, providing global information on an individual's biological state. Currently
64 blood-based biomarkers to assess overall vulnerability in aging are constructed from
65 molecular markers and based on chronological age, disease onset and mortality [3]. Here we
66 focus on data from metabolomics and proteomics platforms representing such novel
67 molecular markers.

68 Proton nuclear magnetic resonance ($^1\text{H-NMR}$) metabolomics enables a cost-effective and
69 standardized assessment of a multitude of small circulating metabolites. Recent extensive
70 collaborative efforts, like BBMRI-NL [4], FINSK/THL [5], COMETS [6], and the UK-Biobank [7],
71 resulted in large datasets generated on the same Nightingale Health PI $^1\text{H-NMR}$
72 metabolomics platform. This platform has been largely explored as a source for generating
73 markers associated with a multitude of endpoints (e.g., type 2 diabetes [8], aging [4], risk
74 factors [9], and disease onset [10]). It gained particular attention, after training the
75 MetaboHealth score, using mortality as endpoint, in the largest study of its kind so far
76 (44,000 individuals and 5,500 incident deaths) [11]. This score stratifies mortality risk with a
77 higher accuracy than conventional clinical variables, with lower and higher values indicating

78 low and higher 5 years risk for mortality, respectively. The MetaboHealth score, though
79 originally trained on mortality outcome, predicts multiple conditions related to overall
80 health decline associated with ageing, such as frailty [12], cognitive decline [13], cancer, as
81 well as respiratory deficiencies [7]. Remarkably, the MetaboHealth score includes only 14
82 metabolic markers. These are involved in processes like glycolysis, fatty acid metabolism,
83 lipoproteins, and inflammation, e.g., GlycA. Although the MetaboHealth score offers an
84 indication on physiological vulnerability, especially for older individuals, it remains largely
85 illusive which pathophysiological mechanisms and corresponding blood factors are tracked
86 by this mortality-trained risk score.

87 To address this question, we performed profiling of proteins and cytokines in serum to
88 explore which molecular pathways co-vary with the MetaboHealth score. To this end, we
89 tested for differences in plasma protein profiles of 50 out of 2200 Leiden Longevity Study
90 participants (mean age~ 56 y.o.) with the most extreme low and high values of
91 MetaboHealth; similarly 50 out of 2900 Rotterdam Study participants (mean age~ 67 y.o.),
92 and 50 monozygotic twins (MZTs) from the 25 most discordant MetaboHealth scoring pairs
93 out of 2,754 twins in the Netherlands Twin Register (mean age~ 36 y.o.). Considering that
94 MZTs have identical genomes, their within-pair associations are free of genetic confounding
95 [14]. Therefore, while the first two cohorts offer an insight into population associations, the
96 MZTs differences inform to what extent MetaboHealth differences in the plasma proteins
97 and cytokines are unconfounded by shared genetics and environment. Overall, our
98 exploration leads to a better understanding of the predictive power of the MetaboHealth
99 score.

100 RESULTS

101 Description of the dataset and study population

102 We performed a nested case-control study design [15], selecting 50 participants with
103 extreme MetaboHealth scores (MetaboHealth), 25 with high score and 25 with low score,
104 from the middle-aged cohort Leiden-Longevity-Study Partners-Offspring (LLS_PAROFFS,
105 mean age~ 56 y.o.), and the Rotterdam Study (RS, mean age~ 67 y.o.) composed by older
106 aged individuals (Figure 1B and Supplementary Table). To minimize potential confounding,
107 we ensured that the lower extreme samples were age- and sex-matched, with at least one
108 high MetaboHealth case (Figure 1A-B). Given that a high MetaboHealth score corresponds to
109 higher mortality risk and poor health status, we categorized individuals with high scores as
110 “cases” and the remainder as “controls”. These disparities in scores are manifested also in
111 phenotypic characteristics. We observed that the cases show significantly higher BMI in
112 LLS_PAROFFS (cases: 26.53 vs controls: 24.37 kg/m²) and a higher incidence of
113 antihypertensive medication in RS (cases: 15 vs controls: 6 users) (Supplementary Table S1).
114 We observed in both study samples a lower level of lymphocyte percentage in the cases (RS:
115 cases= 25.58% vs controls= 35.24%, LLS_PAROFFS: cases=24.72% vs controls= 31.52%)
116 (Figure 1B). Interestingly, cases and controls shared similar phenotypic characteristics,
117 despite being derived from two independent cohorts, differing for the significantly higher
118 ages in RS (mean (age)_{RS} = 74 y.o., mean (age)_{LLS-PAROFFS} = 59 y.o.), accompanied by a slightly
119 elevated BMI in RS (mean (BMI)_{RS} = 25.86, mean (BMI)_{LLS-PAROFFS} = 24.86) and most
120 importantly the larger MetaboHealth contrast in RS (mean (MetaboHealth contrast)_{RS} = 2.4,
121 mean (MetaboHealth contrast)_{LLS-PAROFFS} = 1.7) (Figure 1B, Supplementary Table S1).

122 To investigate to what extent associations between proteins and MetaboHealth scores
123 reflect confounding by shared genetic or environmental factors, we investigated the contrast
124 in MetaboHealth discordant monozygotic twins (MZTs) from the Netherland Twin Register
125 dataset (NTR, mean age~ 36 y.o.) (Figure 1A). 25 Twin pairs with the highest discordance
126 with respect to their MetaboHealth score were selected from 2,754 NTR participants. In
127 accordance with the observations in RS and LLS, the individuals with higher MetaboHealth
128 exhibited a significant reduction in the lymphocyte percentage (cases: 31.37% vs controls:
129 38.64%). Nonetheless, the NTR shows some relevant characteristics when compared to the
130 other two studies. It represents the youngest population, with a 20-year gap
131 (mean(age)_{NTR}=36 y.o.), it has a larger presence of females (36 out of 50), for which the
132 MetaboHealth previously showed a reduced accuracy [16]. These differences, and the
133 selection criterium based on the twin discordancy, possibly lead to a diminished contrast in
134 MetaboHealth values (mean (MetaboHealth contrast)_{NTR}= 1.18) (Figure B).

135

136 **Luminex cytokine assays: higher levels of GDF15, IL6, and MIG in the** 137 **participants with a high MetaboHealth score**

138 To explore the inflammatory state variation between the MetaboHealth extremes, we
139 quantified 15 cytokines on the Luminex platform (Materials and Methods for a complete
140 explanation). Six out of the 15 (40%) cytokines (IL2, TRAIL, GRO1a, IFNg, ILb, and PAI1) were
141 below the detection threshold in most samples, likely implying that the participants were
142 relatively healthy at the time of sampling (Figure 2A and S1). Indeed, on average, more
143 cytokines go undetected in low MetaboHealth participants across the LLS and RS cohorts,
144 hinting at their overall lower inflammation rate (Figure 2A). This discrepancy in detectability

145 attains statistical significance in the case of IL6 (p-value=0.001) (Figure 2A). The same
146 distinctive patterns between the high and low MetaboHealth score cohorts can be observed
147 when considering the two cohorts separately (Figure S1 B-C).

148 Our subsequent analyses focused on nine cytokines (MIP1a, IL6, RANTES, MIG, MCP1,
149 Eotaxin, Psel, GDF15, and BDNF) exhibiting the fewest detectability issues (Figure 2A). We
150 assessed differential expression of these cytokines between MetaboHealth cases and
151 controls, based on a univariate linear regressions corrected for age, and sex as fixed effects.
152 Interestingly, significantly higher levels of GDF15 (estimate~1.08, $fdr=3.9 \times 10^{-8}$), IL6
153 (estimate~1.05, $fdr=1.8 \times 10^{-4}$), and MIG (estimate~0.95, $fdr=1.23 \times 10^{-3}$) were observed in
154 the high MetaboHealth group when considering LLS_PAROFFS and RS together (Figure 2B).
155 Adjusting for medication usage (blood pressure lowering and statins) and cell count
156 (particularly lymphocyte %) influenced mostly the association with GDF15 (Figure S2A-D),
157 yet it remained significant. Finally, reproducing the univariate associations separately for the
158 two cohorts shows similar patterns (Figure S2F), underpinning their robustness.

159 To further investigate the origin of the observed signal, we looked into the correlation
160 structure between cytokines. The generally modest intercorrelation showed a profile of
161 mostly independent features (Figure S2E). Next, we estimated the correlation of the
162 cytokines with the metabolomics components of the MetaboHealth score (Figure 2C). While
163 MetaboHealth exhibits the highest correlations, we observed several noteworthy relations,
164 i.e. strong positive correlations between Glycoprotein Acetyls (GlycA), a metabolomics
165 inflammation marker, and GDF15 ($r=0.33$, $p=8.2 \times 10^{-4}$), MIG ($r=0.27$, $p=7.5 \times 10^{-3}$), and IL6
166 ($r=0.33$, $p=1.9 \times 10^{-3}$). Intriguingly, GDF15 displayed also elevated positive correlations with
167 glucose ($r=0.35$, $p=4.2 \times 10^{-4}$), phenylalanine ($r=0.35$, $p=3.0 \times 10^{-3}$), and isoleucine ($r=0.23$,
168 $p=2.1 \times 10^{-2}$). In contrast, we uncovered prominent negative correlations between GDF15

169 and S-HDL-L (total lipids in small HDL) ($r=-0.38$, $p= 9.9 \times 10^{-5}$), and between MIG and Histidine
170 ($r=-0.33$, $p= 8.7 \times 10^{-4}$).

171

172 **Plasma proteomics associated with extremes in MetaboHealth are**
173 **enriched for inflammatory response and cholesterol transport pathways**

174 In the two population-based samples (50 cases and 50 controls), we investigated plasma
175 proteome profiles by a DIA-based quantitative plasma proteomics pipeline [17,18]
176 (Materials and Methods). 261 out of 337 measured plasma proteins (77%) passed the
177 detection limit and quality control criteria (detailed in Materials and Methods). We
178 identified 106 (68 negative and 38 positive) significant univariate linear associations with the
179 MetaboHealth extremes, adjusted for age, sex, and BMI (Figure 3A). APOA1 (estimate \sim -1.46,
180 $fdr=2.44 \times 10^{-13}$), APOA2 (estimate \sim -1.4, $fdr= 4.02 \times 10^{-12}$), TETN (estimate \sim -1.31, $fdr= 6.42 \times$
181 10^{-11}), GELS (estimate \sim -1.26, $fdr= 3.18 \times 10^{-10}$), and APOA4 (estimate \sim -0.93, $fdr= 5.71 \times 10^{-6}$)
182 were the strongest negative associated proteins. In contrast, the positive acute phase
183 proteins CRP (estimate \sim 1.51, $fdr= 5.81 \times 10^{-14}$), LBP (estimate \sim 1.35, $p= 1.88 \times 10^{-11}$), HPT
184 (estimate \sim 1.14, $p= 1.74 \times 10^{-8}$), were the strongest positive associated proteins. In line with
185 what was observed for the cytokines, the additional correction for medication usage had
186 minimal impact on the univariate associations, while lymphocyte percentage exhibited a
187 slightly more pronounced influence (Figure S4B-D). Furthermore, a meta-analysis to
188 evaluate the associations separately in the two cohorts revealed alike results, with generally
189 stronger signals in the RS (Figure S5 A-B).

190 Subsequently, we explored the statistical interrelations and biological functionalities of
191 the 106 plasma proteome features that exhibited significant association to the

192 MetaboHealth extremes. These proteins showed high correlations with GlycA, comparable
193 to those observed for the MetaboHealth score (Figure S6A). Moreover, within the group of
194 positively associated proteins, smaller clusters of highly correlated proteins are found (Figure
195 S6B). To gain some biological interpretation, we employed KEGG and Gene Ontology to
196 perform functional enrichments separately for the positively and negatively associated
197 proteins (Figure S7). As expected, considering that lower MetaboHealth values are related to
198 healthier metabolic profiles, the negatively associated proteins demonstrated high
199 enrichments for processes relating to “cholesterol transport”, “cholesterol metabolism”, and
200 “high-density lipoproteins particle remodeling” (Figure 3B, S7C and S7E). Conversely, the
201 positively associated proteins were more enriched with “Inflammatory response”,
202 “complement and coagulation cascades”, and intriguingly, “Coronavirus disease” (Figure 3B,
203 S7D and S7F). The latter can be interpreted as a validation, as a subset of about a dozen of
204 inflammation related features, measured with the same proteomics platform, were
205 previously linked to COVID19 outcome [18]. Four of these twelve COVID related plasma
206 proteins exhibited consistently statistically significant differences between the extremes of
207 the MetaboHealth score in RS and LLS-PAROFFs (Figure S8).

208

209 **Genetic influences on the MetaboHealth score and analysis of plasma** 210 **proteins in extreme discordant MZ twins**

211 The NTR has collected 726 complete monozygotic twin (MZTs) and 450 dizygotic twins
212 (DZTs) twin pairs with metabolomics data. We estimated the resemblance in MetaboHealth
213 score as a function of zygosity in these pairs. The correlation between MZ twin pairs was
214 estimated as $r = 0.432$ (95% CI = 0.370-0.489), and the correlation in DZTs was $r = 0.230$ (95%

215 CI = 0.141-0.316), indicating the MetaboHealth score as a heritable trait ($h^2 = 0.4$) (detailed
216 information in Materials and Methods) [19].

217 To exclude potential confounding from genetic factors within our associations, we
218 conducted a monozygotic twin (MZTs) discordant twin pairs design; i.e., high and low scoring
219 MetaboHealth genetically matched twins. In this design an observed effect is not
220 confounded by genetic factors. Therefore, from the total population of MZ twin pairs, we
221 selected a subsample of 25 most discordant MZ twin pairs to further explore associations of
222 the score to the Luminex based cytokines and Mass Spectrometry-base proteomics profiling.
223 Concordantly with the previous sections, the protein markers with the strongest associations
224 with the MetaboHealth score also show a clear separation between cases and controls in the
225 NTR dataset, albeit less than in the LLS and RS studies (Figure 4, and S11). To take advantage
226 of the genetic similarity of the MZ individuals, we tested for associated proteins using a
227 linear mixed model (Methods). The cytokines did not show significant differences in this
228 within-pairs design, although we observed similar trends to the results in LLS and RS, with
229 elevated cytokines in twins with high MetaboHealth scores (Figure S10A). The proteomics
230 analyses revealed a robust signal, identifying a total of 86 significant associations (Figure
231 S10B). Notably, CRP (estimate \sim 1.19, $fdr = 3.75 \times 10^{-5}$) and LBP (estimate \sim 1.15, $fdr = 8.39 \times 10^{-5}$)
232 once again emerged as the most prominently positively associated proteins, while TETN
233 (estimate \sim -1.2, $fdr = 9.69 \times 10^{-5}$) and GELS (estimate \sim -1.11, $fdr = 4.43 \times 10^{-5}$) were confirmed as
234 the most negatively associated proteins. Moreover, the lower associations of APOA1 and
235 APOA2 in the twins' profiles differs from the contrast in LLS and RS and suggests the
236 presence of genetic confounding in the associations between these proteins and the
237 MetaboHealth scores. A correction for health factors had similar results as for the other two
238 cohorts, with lymphocyte percentage having the highest effect (Figure S10C-D).

239 When comparing the NTR associations with the ones observed between the extremes in
240 the other populations, we observed a decrease in signal but maintained a high consistency
241 in the direction of associations (Figure 4). Specifically, 22 positively and 46 negatively
242 associating proteins were in common with the results in RS and LLS-PAROFFs (Figure 4).
243 These results strengthen the reliability of our previous findings indicating that the
244 MetaboHealth score is highly informative on the overall health status of individuals, and
245 finally that a part of its associations with protein levels in extreme individuals can be
246 explained by genetic pleiotropy, i.e. genetic factors influencing both omics traits.

247 **DISCUSSION**

248 The MetaboHealth score, along with other ¹H-NMR metabolomics-based markers,
249 displays risk stratification across a spectrum of health and disease outcomes relevant in
250 ageing research. The score, though based on mortality, has shown to be an indicator of
251 overall health status in middle and older aged individuals. Within this context, our study set
252 out to quantify comprehensive plasma proteome profiles in 150 samples at the extreme
253 ends of the MetaboHealth distributions from three large Dutch cohorts (Leiden Longevity
254 Study, Rotterdam Study, and the Netherlands Twin Register, spanning a total dataset of
255 7,854 individuals). Our findings revealed significant differential expression among 106
256 plasma proteins and 3 cytokines markers, consistently observed in the RS and LLS-PAROFFs,
257 between the highest (cases) and the lowest (controls) MetaboHealth scores, respectively
258 indicating elevated and reduced mortality risk. These associations were for the majority not
259 confounded by age, sex, BMI, and medication usage. A part of the proteins associated with
260 the MetaboHealth contrast could be explained by genetic confounding as demonstrated by
261 investigating discordant monozygotic twins.

262 The majority of the significant associations (68 out of 106) resulted in negatively
263 associated proteins with the case/control contrast, indicating higher protein levels in
264 samples of healthier subjects (reflected by lower MetaboHealth scores). Functional
265 enrichment of these proteins revealed associations with healthy metabolism, particularly in
266 high-density lipoprotein (HDL) remodeling and cholesterol transport pathways. Notably, the
267 most prominent associated proteins were APOA1 and APOA2, crucial components of HDL
268 and widely recognized as protective markers for cardiovascular disease [20,21]. It should be
269 noted that likely a substantial genetic component drives APOA1 and 2b, since these proteins

270 were significantly less discordant in the MetaboHealth discordant MZ twins. This aspect
271 must be further investigated since a genetic component may be overestimated given that
272 the MetaboHealth contrast in the (overall younger) MZ twins was rather small in comparison
273 to the cohort studies. Interestingly, the associations with tetranectin (TETN) and gelsolin
274 (GELS) emerged as consistently stable also in NTR. Both these proteins are under
275 consideration as potential protective markers for various diseases, such as cancer,
276 cardiovascular disease and neurodegeneration [22–24].

277 We also observed several relevant proteins that were significantly positively associated
278 with the MetaboHealth contrast. The cytokine markers selected for this study were
279 previously reported to strongly associate with frailty, ageing, age-related disease, and
280 mortality [25–28]. While a large part of the cytokines could not be efficiently detected,
281 which can be attributed to the absence of ongoing infections and acute inflammation at
282 blood sampling, GDF15, IL6, and MIG (gene name=CXCL9), showed significant associations
283 with higher MetaboHealth levels. These cytokines serve different roles in the body and are
284 involved in cell signalling immune response, and inflammation. All three markers are
285 potential biomarkers for aging-related physiological decline and frailty, where IL6 marks
286 chronic inflammation (“inflammaging”) [29–32]; GDF-15 is a senescence associated
287 secretory protein (SASP) and a marker of physiological stress response and mitochondrial
288 dysfunction and MIG is the most prominent marker emerging from the inflammatory aging
289 clock (see materials and Methods) [25]. In this regard, also the 38 significantly positively
290 associated plasma proteins are predominantly involved in inflammatory response,
291 complement and coagulation cascades, and COVID19. CRP, HPT and LBP, well-known
292 biomarkers assessing the degree of inflammation and immune response, displayed the
293 highest significant associations.

294 Interestingly the inflammatory component in the positively associated markers also links
295 to COVID19 infection pathways, regardless of their infection status, considering that blood
296 samples used in this study were drawn up to 15 years before the COVID19 pandemic.
297 Noteworthy is that both the proteomics panel and the metabolomics assay composing the
298 MetaboHealth score in plasma, were previously observed to be able to stratify severe cases
299 of COVID19 [7,18]. Several plasma proteins previously related to COVID19 were significantly
300 different also in our MetaboHealth contrast in at least one study. These include the inter- α -
301 trypsin inhibitors family, ITIH1, ITIH2, respectively positively and negatively associated, and
302 HRG, LCAT, which are both positively associated to MetaboHealth (Figure S8A).

303 Significant disparities in phenotypic characteristics were observed between cases and
304 controls across the cohorts, mostly in the higher levels of BMI and antihypertensive usage
305 respectively in LLS and RS. However, of great importance from a health perspective seemed
306 to be the significant reduction of lymphocyte percentage consistently among the cases in all
307 studies, although still within healthy ranges (20-40%). Concordantly, the systematic
308 adjustment for health and risk factors (age, sex, BMI, lymphocyte and monocyte %, lipid and
309 antihypertensive medication usage) resulted in an attenuation of the signal to 89/106
310 plasma proteins and 3/3 cytokines, with the strongest effect being related to the lymphocyte
311 percentage (Figure S4A-D). Interestingly, a decrease in lymphocyte counts and increased
312 cytokine in blood is frequently related to a decline in immune system functions that
313 accompanies physiological aging [33–36]. Considering the age matching within our study
314 inclusion criteria, these observations suggest that the MetaboHealth score successfully
315 identified individuals with accelerated biological aging given their chronological age. While
316 the correction for cell counts partially accounted for the observed signal, it was evident that
317 hematopoietic variation alone does not explain the observed MetaboHealth contrast in

318 plasma proteins. Consequently, further investigation is required to elucidate whether
319 MetaboHealth and cell count percentages can jointly be more informative in indicating
320 health status of older individuals and secondly what the relation with these parameters and
321 inflammation is. .

322 Conducting heritability analyses within the Netherlands Twin Register allowed us to
323 establish that the MetaboHealth score has a heritability of ~40%, at least in relatively
324 younger ages (mean age~36 y.o.). Therefore, the Monozygotic twin subset provided an ideal
325 setting to further examine the proteomics associations within a genetically identical
326 population. Cytokines did not exhibit significant associations to the MetaboHealth contrast
327 in the twins, while we found up to 46 negative and 22 positive plasma protein relations. An
328 attenuation of the number and strength of associations indicate that part of the signal may
329 be explained by genetic factors that influence both the MetaboHealth score and quantified
330 proteins. Further research should be focused on investigating the genetic confounding in
331 twins of higher ages where MetaboHealth is even more informative. Pertaining to this, it is
332 essential to highlight that NTR participants had lower MetaboHealth contrasts as they are
333 younger of age as well as due to the inclusion restriction. Supposedly for the same reasons,
334 diminished associations are noted also when comparing the results in LLS-PAROFFs to RS
335 (Figures S5). Possibly as individuals age, environmental and/or stochastic factors gain
336 greater importance on the features included in the MetaboHealth score over genetic
337 influences.

338 One aspect of our study that can be regarded as a limitation is the generally healthy state
339 of the participants in the cohorts from which we derived our participants. Consequently, the
340 observed contrast between the extreme levels of MetaboHealth was relatively modest. This
341 is underscored by the fact that several of the examined cytokines consistently fell under the

342 detection limit, a circumstance that can be largely attributed to the overall absence of
343 ongoing infections at blood sampling which proteins may be useful biomarkers in clinical
344 studies. We envision MetaboHealth as a score potentially giving an indication of vulnerability
345 in individuals from the population in a modifiable health phase, way before onset and
346 diagnosis of specific diseases. The score indeed effectively identified relevant biological
347 differences within all three populations indicating that early changes in multiple metabolic
348 and proteome parameters known to reflect decline in health is represented by the score.
349 Given the limited number of individuals in our selection we do not have the statistical power
350 to explore concrete endpoints such as mortality or frailty in this study. We consider this
351 study as a proof of principle design to explore the relevance of omics scores generated in the
352 ageing field in the context of additional omics levels, to better understand why a score
353 predicts endpoints and by what parameters the predictive power may potentially be
354 improved.

355 In conclusion, our study confirms MetaboHealth as a robust marker for the inflammatory
356 aspects of aging. In accordance with the current biological aging theories, this score
357 effectively identifies individuals exhibiting reduced lymphocyte counts and increased levels
358 of pro-inflammatory proteins regardless of chronological aging. We believe that this
359 investigation supports integrating the MetaboHealth score with proteome data to enhance
360 the prognostic value of the score, increase our comprehension of the aging process and loss
361 of health in individuals identified by the score and the health gain that may be expected by
362 timely intervention.

363

364 **MATERIALS AND METHODS**

365 **Study design**

366 This study was actuated starting from the metabolomics data included in the BBMRI-NL
367 consortium originated from the participants to three cohorts: Leiden Longevity Study (LLS-
368 PAROFFS), Rotterdam Study (RS), and the Netherlands Twin Register (NTR). The Leiden
369 Longevity study is a population-based cohort with a unique two-generation design,
370 examining 421 Dutch long-lived families [37]. The current work was performed on the first
371 measurements (IOP1) of the second generation, namely the Offspring and their Partners, for
372 a total of 2,313 participants. The Rotterdam Study is a population-based prospective study
373 on individuals living in a specific neighborhood in Rotterdam, prone to cardiovascular
374 endpoints [38]. The current study was set off utilizing the first measurements (RS-I), which
375 enclosed a total of 2,986 participants. The Netherlands Twin Register is a prospective study
376 investigating young and adult twins and multiples along with their family members. In this
377 particular study we focused on the monozygotic dizygotic twin pairs within in the cohort, for
378 heritability estimation and implemented a within pairs case-control study design for the 25
379 most discordant MZ twin pairs.

380

381 **Data and sample collection**

382 **Metabolomics measurements**

383 The metabolomics dataset was generated by the BBMRI-NL Consortium on the EDTA
384 plasma samples of the entire cohorts (LLS-PAROFFS: 2,313 samples, RS: 2,986 samples, and
385 NTR: samples). The features were quantified using the high-throughput proton Nuclear
386 Magnetic Resonance ($^1\text{H-NMR}$) platform made available by Nightingale Health Ltd., Helsinki,

387 Finland. This technique can quantify over 230 metabolic features in a single assay, including
388 lipids, lipoproteins, fatty acid composition, various amino acids, and their derived measures
389 (e.g., ratios) [39,40]. We employed the dataset quantified in 2014 to ensure the correct
390 projection of the MetaboHealth model, originally trained on this version of the platform.

391

392 **Selection of the participants from the large population studies**

393 **LLS-PAROFFS and RS:** The sample selection was based on the chronological age
394 independent part of the MetaboHealth, which was obtained as the residual from a linear
395 regression of chronological age on the metabolomics score. The cases were defined as the
396 25 participants with the highest MetaboHealth, indicating an unhealthier status, within each
397 cohort separately. Following, to limit the confounding effect of sex and age, the controls
398 were selected as the participants with the lowest score that could have at least one match
399 with the cases in terms of both age, and sex.

400 **NTR:** The twin population of NTR was composed on 726 complete monozygotic (MZTs)
401 and 450 complete dizygotic (DZTs) twin pairs. We extracted the 25 twin pairs which showed
402 the largest differences in MetaboHealth score.

403

404 **Cytokines quantification**

405 We used previously validated multiplex immunoassays (Luminex platform) to determine
406 plasma protein levels [41]. All assays were performed at the ISO-certified multiplex core
407 facility of the UMC Utrecht, Utrecht, The Netherlands. Before analysis all samples were
408 centrifuged through 0.22 μm spin-X filtration columns (Corning, Corning NY USA) to remove
409 debris. Non-specific (heterophilic) antibodies, which may interfere with the assay, were
410 blocked using Heteroblock (Omega Biologicals, Bozeman, MT, USA) as previously described

411 [10,11]. If applicable, samples were diluted in high performance elisa buffer (HPE buffer,
412 Sanquin, Amsterdam, the Netherlands). We determined levels of the immunoregulating
413 proteins IL-1 β , IL-2, IL-6, IFN- γ , GDF-15, CCL2/MCP-1, CCL3/MIP-1 α , CCL5/RANTES,
414 CCL11/Eotaxin, CXCL1/GRO-1 α , CXCL9/MIG, PAI-1, BDNF, TRAIL and soluble P-selectin in
415 plasma. These markers were selected based on two criteria, first that they could be
416 measured on our budgetary boundaries using the Luminex platform in the Utrecht
417 University; secondly because they were previously indicated as markers of ageing, mortality,
418 frailty and age-related disease. The last criterium was in great part based on the following
419 studies: A) belonging to the top 15 most informative variables in the iAge clock [25](for the
420 cytokines: CXCL9/MIG, EOTAXIN, CCL3/Mip-1 α , IL-1 β , IFN- γ , CXCL5/RANTES, CXCL1/GRO-1 α ,
421 CCL2/MCP1, IL-2; TRAIL, PAI-1); B) recognized as indicators of frailty (Pselectin and BDNF)
422 [26]; C) or marker of chronic inflammation (IL6) [27], and d) finally, widely explored marker
423 for aging, cancer, cardiovascular, and lung disease (GDF-15/MIC-1) [28].

424 Although the majority of the features (73%) were quantified in undiluted samples, PAI1
425 was measured with a dilution rate of 1/10, and, GDF15, RANTES, and BDNF, with a dilution
426 rate of 1/100.

427

428 **Protein digestion**

429 Protein digestion was performed on an Agilent Bravo liquid handling Platform following
430 Vollmy et. al. [18]. A pooled QC sample was prepared by pooling an equal amount of each
431 digested sample. Then all samples were diluted 40 times with TFA 1% to bring them to an
432 approximate concentration of 10 ng/ μ L. Finally, the samples were loaded onto Evotips
433 (Odense, Denmark) using an Agilent Bravo liquid handling platform.

434

435 **LC-MS data acquisition**

436 The digested samples were measured using the 60 SPD method of a Evosep One (Odense,
437 Danemark) on a EV-1109 column (C18, 8 cm x 150 μ m, 1.5 μ m, Evosep, Danemark) coupled
438 to a timsTOF-HT (Bruker, Germany) equipped with a Captive Spray source and operating in
439 DIA-PASEF adapted from Skowronek et. al. [42] Briefly, two ion mobility windows per dia-
440 PASEF scan with 12 variable isolation window widths adjusted to the precursor densities
441 were used. The ion mobility range was set to 0.6 and 1.5 cm^{-1} . The accumulation and ramp
442 times were specified as 100 ms for all experiments. Source capillary voltage and
443 temperature were set to 1800 V and 180°C. Drying and sheath gas were set to 3 L/min. The
444 pooled QC samples were injected every 8 samples.

445

446 **Processing of proteomics data**

447 Raw data were processed using DIA-NN 1.8.1 [43], Peptides were searched against an in-
448 silico predicted library computed from the human proteome with isoforms (UniProtKB and
449 TrEMBL, 103830 protein entries and 20560 genes) and the common protein contaminants
450 with 2 missed-cleavages and no variable modification. Match Between Run was used and
451 the Heuristic inference was disabled. MS1 and MSMS mass accuracy were set to 10 and 20
452 ppm respectively.

453 The protein intensities were computed using the maxLFQ algorithm implemented in the
454 DIA-NN R-package. For this only the prototypic precursors that satisfy the following criteria
455 were considered: Q.value \leq 1%, missing value \leq 20% and RSD \leq 40% in the QC samples. The
456 protein groups were filtered at lib.Q.Value \leq 1%, lib.PG.Q.value \leq 1%.

457

458 **Covariates**

459 Data on age (in years), sex (males/females), BMI (kg/m²), cell counts (%), lipid medication,
460 and blood pressure lowering medication were reported within the BBMRI-nl Consortium.
461 These covariates were evaluated as possible confounders as they are known to be associated
462 with both the metabolomics and the proteomics datasets. Age and sex were self-reported,
463 and BMI was calculated based on weight and height. The cell counts percentage was defined
464 as the measured monocytes and lymphocytes percentage, taking the granulocyte
465 percentage as given.

466

467 **Statistical Analyses**

468 **Preprocessing**

469 *Metabolomics and MetaboHealth score projection:* We applied the same quality control
470 previously described by Deelen et al. [11], using the R package MiMIR [44]. While the
471 Nightingale Health platform measures over 250 metabolomics features, we focused our
472 attention on the 14 metabolomics variables included in the MetaboHealth model (list of
473 analytes can be found in the Supplementary Table S1). Then, we applied a logarithm
474 transformation to the analytes, while adding a value of 1 to all analytes containing any zero
475 as a value. Afterwards a z-scale normalization was applied separately within each cohort to
476 minimize batch effects. Finally, we projected the MetaboHealth score using the coefficients
477 indicated by Deelen et al. [11,44].

478 *Cytokines:* Initially, we assessed the occurrence of samples reported as under the lower
479 detection thresholds, comparing cases and controls, separately for each feature.
480 Subsequently, we employed the Fisher test to determine the statistical significance of these

481 difference ($p\text{-value} \leq 0.05$). Following, we proceeded to exclude six out of fifteen features
482 that consistently fell below the lower detection thresholds in most of the quantified samples
483 (namely, IL2, TRAIL, GRO1a, IFNg, IL1b, and PAI1 were undetected in more than 65% of the
484 samples). There were no values recognized as outlier samples, considered as values more
485 than 5 standard deviations (SD) away from the mean of the feature. Finally, the remaining
486 nine features were first log transformed and then z scaled separately per biobank to reduce
487 batch effects.

488 *Proteomics:* We applied a similar approach to the proteomics. We evaluated the
489 differential patterns in missing values of the features between the cases and controls.
490 Features with more than 5% missing values (20 missing) were subsequently excluded,
491 resulting in a set of 261 analytes, from the 337 initial set 8 values (0.03%) were recognized as
492 outliers, meaning that they resulted as the values 5 SD away from their mean of the feature
493 and set as missing information. We imputed the remaining 114 missing values (0.4%) using
494 the non-linear iterative partial least squares method (nipals), implemented in the R package
495 *pcaMethods*. Finally, to enhance comparability and facilitate downstream analysis we
496 performed a log transformation and a z-scaling of the features per biobank.

497

498 **Linear Association and Meta-analyses in RS and LLS-PAROFFS**

499 Initially, we applied linear regression models across the entire dataset to assess the
500 associations between each cytokines and proteomics features separately, with the
501 case/control status of the participants. These analyses accounted for potential confounding
502 factors (age, sex, BMI, cell counts, and usage of lipid medication and blood pressure
503 lowering medication). Subsequently, we attempted to evaluate the associations
504 independently for each cohort (LLS-PAROFFS and RS) and conducted a meta-analysis. The

505 meta-analysis was performed with a restricted maximum likelihood estimator using the
506 package *metafor* in R. To correct for multiple testing, we applied False Discovery Rate (FDR).

507

508 **Enrichment Analyses and Network analysis**

509 We performed the functional enrichment of the most interesting proteomics features
510 using the web-tool *Enrichr* [45]. We evaluated the Gene Ontology (GO) Biological Processes
511 (BP), the KEGG pathways, and Reactome. Firstly, we performed an enrichment analyses on
512 the full set of 337 proteomics features to evaluate the functions overall characterizing to the
513 proteomics platform (Figure S7A-B). Secondly, we analyzed separately the 38 positively and
514 the 68 negatively associated proteins to the MetaboHealth's extremes corrected for sex, age,
515 and BMI (Figure S7C-H). To ensure a fair enrichment analysis of the significantly associated
516 proteins we used the full list of 337 proteins as the background of possible analytes. To
517 better interpret at the GO BP results we used the R package *rrvgo* (threshold=0.7), which is
518 able to summarize the redundant information in the database [46].

519

520 **Analyses in the Netherlands Twin Register**

521 First, we examined heritability of the MetaboHealth score within Netherland Twin
522 Register. Monozygotic twins (MZTs) share their (almost) complete DNA sequence, while
523 dizygotic twins (DZTs) share on average 50% of their segregating genes. Any differences in
524 correlations between MZTs and between DZTs offers a first hint on genetic influences in the
525 signal. We obtained an estimate of the heritability of a trait (h^2) using the formula: $h^2 =$
526 $2(r_{MZTs} - r_{DZTs})$, where r denotes the correlation between the twins [19].

527 Secondly, we assessed the associations between the cytokines and serum protein
528 features with the case/control status of the selected MZTs with the highest MetaboHealth

529 differences. To do this we used linear mixed models to consider the family status, while
530 allowing to systematically correct for potential covariates. Finally, FDR to correct for multiple
531 testing.

532

533 **Data sharing**

534 Mass Spectrometry data have been deposited to the ProteomeXchange Consortium
535 via the PRIDE partner repository with the dataset identifier PXD057946. Phenotypic
536 information are available upon reasonable request at BBMRI-nl
537 <https://www.bbmri.nl/services/samples-images-data>.

538 **Acknowledgements**

539 This work was performed within the BBMRI Metabolomics Consortium funded by:
540 BBMRI-NL (financed by NWO 184.021.007 and 184.033.111), X-omics (NWO 184.034.019),
541 VOILA (ZonMW 457001001) and Medical Delta (METABODELTA: Metabolomics for clinical
542 advances in the Medical Delta). EvdA is funded by a personal grant of the Dutch Research
543 Council (NWO; VENI:09150161810095). Acknowledgements for all contributing studies can
544 be found in the Supplementary Material-BIOS Consortium. Finally, we would like to thank
545 Prof. Peter Bram 't Hoen for critically appraising this manuscript.

546 **Contributors**

547 PES, DB, EbvDA, and MJTR conceived and wrote the manuscript. DB performed the
548 analyses. EBvDA and MJTR verified and supervised the analyses. PES, MB, DiB, AjvG, DB,
549 EbvDA, and MJTR were involved in defining the study design. PES, MB, and NL were involved
550 in the data acquisition for the LLS-PAROFF cohort; RP and DiB in the data acquisition of the
551 Netherland Twin Register; JmV and MG in the data acquisition of the Rotterdam Study. AjrH,

552 ND, and KeS performed the Mass Spectrometry proteomics. EFK performed the cytokine
553 quantification. All authors discussed the results and contributed to the final manuscript.

554 **Competing Interests**

555 Authors declare no competing interests.

556 **REFERENCES**

- 557 1. Partridge, L.; Deelen, J.; Slagboom, P.E. Facing up to the Global Challenges of Ageing.
558 *Nature* **2018**, *561*, 45–56, doi:10.1038/s41586-018-0457-8.
- 559 2. Comfort, A. TEST-BATTERY TO MEASURE AGEING-RATE IN MAN. *The Lancet* **1969**, *294*,
560 1411–1415, doi:10.1016/S0140-6736(69)90950-7.
- 561 3. Moqri, M.; Herzog, C.; Poganik, J.R.; Biomarkers of Aging Consortium; Justice, J.; Belsky,
562 D.W.; Higgins-Chen, A.; Moskalev, A.; Fuellen, G.; Cohen, A.A.; et al. Biomarkers of Aging
563 for the Identification and Evaluation of Longevity Interventions. *Cell* **2023**, *186*, 3758–
564 3775, doi:10.1016/j.cell.2023.08.003.
- 565 4. van den Akker Erik B.; Trompet Stella; Barkey Wolf Jurriaan J.H.; Beekman Marian;
566 Suchiman H. Eka D.; Deelen Joris; Asselbergs Folkert W.; Boersma Eric; Cats Davy; Elders
567 Petra M.; et al. Metabolic Age Based on the BBMRI-NL 1H-NMR Metabolomics
568 Repository as Biomarker of Age-Related Disease. *Circulation: Genomic and Precision*
569 *Medicine* **2020**, *13*, 541–547, doi:10.1161/CIRCGEN.119.002610.
- 570 5. Group, N.H.B.C.; Barrett, J.C.; Esko, T.; Fischer, K.; Jostins-Dean, L.; Jousilahti, P.;
571 Julkunen, H.; Jääskeläinen, T.; Kerimov, N.; Kerminen, S.; et al. Metabolomic and
572 Genomic Prediction of Common Diseases in 477,706 Participants in Three National
573 Biobanks 2023, 2023.06.09.23291213.
- 574 6. Yu, B.; Zanetti, K.A.; Temprosa, M.; Albanes, D.; Appel, N.; Barrera, C.B.; Ben-Shlomo, Y.;
575 Boerwinkle, E.; Casas, J.P.; Clish, C.; et al. The Consortium of Metabolomics Studies
576 (COMETS): Metabolomics in 47 Prospective Cohort Studies. *Am J Epidemiol* **2019**, *188*,
577 991–1012, doi:10.1093/aje/kwz028.
- 578 7. Nightingale Health UK Biobank Initiative; Julkunen, H.; Cichońska, A.; Slagboom, P.E.;
579 Würtz, P. Metabolic Biomarker Profiling for Identification of Susceptibility to Severe
580 Pneumonia and COVID-19 in the General Population. *eLife* **2021**, *10*, e63033,
581 doi:10.7554/eLife.63033.
- 582 8. 't Hart, L.M.; Vogelzangs, N.; Mook-Kanamori, D.O.; Brahimaj, A.; Nano, J.; van der
583 Heijden, A.A.W.A.; Willems van Dijk, K.; Slieker, R.C.; Steyerberg, E.W.; Ikram, M.A.; et al.
584 Blood Metabolomic Measures Associate With Present and Future Glycemic Control in
585 Type 2 Diabetes. *The Journal of Clinical Endocrinology & Metabolism* **2018**, *103*, 4569–
586 4579, doi:10.1210/jc.2018-01165.
- 587 9. Bizzarri, D.; Reinders, M.J.T.; Beekman, M.; Slagboom, P.E.; Bbmri, N.; van den Akker,
588 E.B. 1H-NMR Metabolomics-Based Surrogates to Impute Common Clinical Risk Factors
589 and Endpoints. *EBioMedicine* **2022**, *75*, 103764, doi:10.1016/j.ebiom.2021.103764.
- 590 10. Buerge, T.; Steinfeldt, J.; Ruyoga, G.; Pietzner, M.; Bizzarri, D.; Vojinovic, D.; Upmeier zu
591 Belzen, J.; Loock, L.; Kittner, P.; Christmann, L.; et al. Metabolomic Profiles Predict
592 Individual Multidisease Outcomes. *Nat Med* **2022**, *28*, 2309–2320, doi:10.1038/s41591-
593 022-01980-3.

- 594 11. Deelen, J.; Kettunen, J.; Fischer, K.; van der Spek, A.; Trompet, S.; Kastenmüller, G.;
595 Boyd, A.; Zierer, J.; van den Akker, E.B.; Ala-Korpela, M.; et al. A Metabolic Profile of All-
596 Cause Mortality Risk Identified in an Observational Study of 44,168 Individuals. *Nature*
597 *Communications* **2019**, *10*, 1–8, doi:10.1038/s41467-019-11311-9.
- 598 12. Kuiper, L.M.; Polinder-Bos, H.A.; Bizzarri, D.; Vojinovic, D.; Vallerga, C.L.; Beekman, M.;
599 Dollé, M.E.T.; Ghanbari, M.; Voortman, T.; Reinders, M.J.T.; et al. Epigenetic and
600 Metabolomic Biomarkers for Biological Age: A Comparative Analysis of Mortality and
601 Frailty Risk. *The Journals of Gerontology: Series A* **2023**, glad137,
602 doi:10.1093/gerona/glad137.
- 603 13. Zonneveld, M.H.; Kuhaili, N.A.; Mooijaart, S.P.; Slagboom, P.E.; Jukema, J.W.; Noordam,
604 R.; Trompet, S. Increased 1H-NMR Metabolomics-Based Health Score Associates with
605 Declined Cognitive Performance and Functional Independence in Older Adults at Risk
606 of Cardiovascular Disease 2023, 2023.12.21.23300037.
- 607 14. Gonggrijp, B.M.A.; van de Weijer, S.G.A.; Bijleveld, C.C.J.H.; van Dongen, J.; Boomsma,
608 D.I. The Co-Twin Control Design: Implementation and Methodological Considerations.
609 *Twin Res Hum Genet* **2023**, 1–8, doi:10.1017/thg.2023.35.
- 610 15. Ernster, V.L. Nested Case-Control Studies. *Preventive Medicine* **1994**, *23*, 587–590,
611 doi:10.1006/pmed.1994.1093.
- 612 16. Bizzarri, D.; Reinders, M.J.T.; Kuiper, L.M.; Beekman, M.; Deelen, J.; Meurs, J.B.J. van;
613 Dongen, J. van; Pool, R.; Boomsma, D.I.; Ghanbari, M.; et al. 1H-NMR Metabolomics-
614 Guided DNA Methylation Mortality Predictors 2023, 2023.11.02.23297956.
- 615 17. Geyer, P.E.; Kulak, N.A.; Pichler, G.; Holdt, L.M.; Teupser, D.; Mann, M. Plasma Proteome
616 Profiling to Assess Human Health and Disease. *Cell Syst* **2016**, *2*, 185–195,
617 doi:10.1016/j.cels.2016.02.015.
- 618 18. Völlmy, F.; van den Toorn, H.; Zenezini Chiozzi, R.; Zucchetti, O.; Papi, A.; Volta, C.A.;
619 Marracino, L.; Vieceli Dalla Sega, F.; Fortini, F.; Demichev, V.; et al. A Serum Proteome
620 Signature to Predict Mortality in Severe COVID-19 Patients. *Life Sci Alliance* **2021**, *4*,
621 e202101099, doi:10.26508/lsa.202101099.
- 622 19. Boomsma, D.; Busjahn, A.; Peltonen, L. Classical Twin Studies and Beyond. *Nat Rev*
623 *Genet* **2002**, *3*, 872–882, doi:10.1038/nrg932.
- 624 20. Florvall, G.; Basu, S.; Larsson, A. Apolipoprotein A1 Is a Stronger Prognostic Marker than
625 Are HDL and LDL Cholesterol for Cardiovascular Disease and Mortality in Elderly Men. *J*
626 *Gerontol A Biol Sci Med Sci* **2006**, *61*, 1262–1266, doi:10.1093/gerona/61.12.1262.
- 627 21. Sato, Y.; Kobayashi, T.; Nishiumi, S.; Okada, A.; Fujita, T.; Sanuki, T.; Kobayashi, M.;
628 Asahara, M.; Adachi, M.; Sakai, A.; et al. Prospective Study Using Plasma Apolipoprotein
629 A2-Isoforms to Screen for High-Risk Status of Pancreatic Cancer. *Cancers (Basel)* **2020**,
630 *12*, 2625, doi:10.3390/cancers12092625.
- 631 22. Bucki, R.; Levental, I.; Kulakowska, A.; Janmey, P.A. Plasma Gelsolin: Function,
632 Prognostic Value, and Potential Therapeutic Use. *Curr Protein Pept Sci* **2008**, *9*, 541–
633 551, doi:10.2174/138920308786733912.
- 634 23. Li, G.H.; Arora, P.D.; Chen, Y.; McCulloch, C.A.; Liu, P. Multifunctional Roles of Gelsolin in
635 Health and Diseases. *Med Res Rev* **2012**, *32*, 999–1025, doi:10.1002/med.20231.
- 636 24. McDonald, K.; Glezeva, N.; Collier, P.; O'Reilly, J.; O'Connell, E.; Tea, I.; Russell-Hallinan,
637 A.; Tonry, C.; Pennington, S.; Gallagher, J.; et al. Tetranectin, a Potential Novel
638 Diagnostic Biomarker of Heart Failure, Is Expressed within the Myocardium and
639 Associates with Cardiac Fibrosis. *Sci Rep* **2020**, *10*, 7507, doi:10.1038/s41598-020-
640 64558-4.

- 641 25. Sayed, N.; Huang, Y.; Nguyen, K.; Krejciova-Rajaniemi, Z.; Grawe, A.P.; Gao, T.; Tibshirani,
642 R.; Hastie, T.; Alpert, A.; Cui, L.; et al. An Inflammatory Aging Clock (iAge) Based on
643 Deep Learning Tracks Multimorbidity, Immunosenescence, Frailty and Cardiovascular
644 Aging. *Nat Aging* **2021**, *1*, 598–615, doi:10.1038/s43587-021-00082-y.
- 645 26. Samson, L.D.; Buisman, A.; Ferreira, J.A.; Picavet, H.S.J.; Verschuren, W.M.M.; Boots,
646 A.M.; Engelfriet, P. Inflammatory Marker Trajectories Associated with Frailty and Ageing
647 in a 20-year Longitudinal Study. *Clin Transl Immunology* **2022**, *11*, e1374,
648 doi:10.1002/cti2.1374.
- 649 27. Franceschi, C.; Bonafè, M.; Valensin, S.; Olivieri, F.; De Luca, M.; Ottaviani, E.; De
650 Benedictis, G. Inflamm-Aging. An Evolutionary Perspective on Immunosenescence. *Ann*
651 *N Y Acad Sci* **2000**, *908*, 244–254, doi:10.1111/j.1749-6632.2000.tb06651.x.
- 652 28. Wischhusen, J.; Melero, I.; Fridman, W.H. Growth/Differentiation Factor-15 (GDF-15):
653 From Biomarker to Novel Targetable Immune Checkpoint. *Front Immunol* **2020**, *11*, 951,
654 doi:10.3389/fimmu.2020.00951.
- 655 29. Liu, H.; Huang, Y.; Lyu, Y.; Dai, W.; Tong, Y.; Li, Y. GDF15 as a Biomarker of Ageing.
656 *Experimental Gerontology* **2021**, *146*, 111228, doi:10.1016/j.exger.2021.111228.
- 657 30. Wan, Y.; Fu, J. GDF15 as a Key Disease Target and Biomarker: Linking Chronic Lung
658 Diseases and Ageing. *Mol Cell Biochem* **2023**, 1–14, doi:10.1007/s11010-023-04743-x.
- 659 31. de Gonzalo-Calvo, D.; Neitzert, K.; Fernández, M.; Vega-Naredo, I.; Caballero, B.; García-
660 Macía, M.; Suárez, F.M.; Rodríguez-Colunga, M.J.; Solano, J.J.; Coto-Montes, A.
661 Differential Inflammatory Responses in Aging and Disease: TNF-Alpha and IL-6 as
662 Possible Biomarkers. *Free Radic Biol Med* **2010**, *49*, 733–737,
663 doi:10.1016/j.freeradbiomed.2010.05.019.
- 664 32. Maggio, M.; Guralnik, J.M.; Longo, D.L.; Ferrucci, L. Interleukin-6 in Aging and Chronic
665 Disease: A Magnificent Pathway. *J Gerontol A Biol Sci Med Sci* **2006**, *61*, 575–584.
- 666 33. Valiathan, R.; Ashman, M.; Asthana, D. Effects of Ageing on the Immune System: Infants
667 to Elderly. *Scand J Immunol* **2016**, *83*, 255–266, doi:10.1111/sji.12413.
- 668 34. Tavares, S.M.Q.M.C.; Junior, W. de L.B.; Lopes e Silva, M.R. Normal Lymphocyte
669 Immunophenotype in an Elderly Population. *Rev Bras Hematol Hemoter* **2014**, *36*, 180–
670 183, doi:10.1016/j.bjhh.2014.03.021.
- 671 35. Yan, J.; Greer, J.M.; Hull, R.; O’Sullivan, J.D.; Henderson, R.D.; Read, S.J.; McCombe, P.A.
672 The Effect of Ageing on Human Lymphocyte Subsets: Comparison of Males and
673 Females. *Immunity & Ageing* **2010**, *7*, 4, doi:10.1186/1742-4933-7-4.
- 674 36. Nikolic-Žugich, J. Ageing and Life-Long Maintenance of T-Cell Subsets in the Face of
675 Latent Persistent Infections. *Nat Rev Immunol* **2008**, *8*, 512–522, doi:10.1038/nri2318.
- 676 37. Schoenmaker, M.; de Craen, A.J.M.; de Meijer, P.H.E.M.; Beekman, M.; Blauw, G.J.;
677 Slagboom, P.E.; Westendorp, R.G.J. Evidence of Genetic Enrichment for Exceptional
678 Survival Using a Family Approach: The Leiden Longevity Study. *European Journal of*
679 *Human Genetics* **2006**, *14*, 79–84, doi:10.1038/sj.ejhg.5201508.
- 680 38. Ikram, M.A.; Brusselle, G.G.O.; Murad, S.D.; van Duijn, C.M.; Franco, O.H.;
681 Goedegebure, A.; Klaver, C.C.W.; Nijsten, T.E.C.; Peeters, R.P.; Stricker, B.H.; et al. The
682 Rotterdam Study: 2018 Update on Objectives, Design and Main Results. *Eur J Epidemiol*
683 **2017**, *32*, 807–850, doi:10.1007/s10654-017-0321-4.
- 684 39. Würtz, P.; Kangas, A.J.; Soininen, P.; Lawlor, D.A.; Davey Smith, G.; Ala-Korpela, M.
685 Quantitative Serum Nuclear Magnetic Resonance Metabolomics in Large-Scale
686 Epidemiology: A Primer on -Omic Technologies. *Am. J. Epidemiol.* **2017**, *186*, 1084–
687 1096, doi:10.1093/aje/kwx016.

- 688 40. Soininen, P.; Kangas, A.J.; Würtz, P.; Suna, T.; Ala-Korpela, M. Quantitative Serum
689 Nuclear Magnetic Resonance Metabolomics in Cardiovascular Epidemiology and
690 Genetics. *Circ Cardiovasc Genet* **2015**, *8*, 192–206,
691 doi:10.1161/CIRCGENETICS.114.000216.
- 692 41. Scholman, R.C.; Giovannone, B.; Hiddingh, S.; Meerding, J.M.; Malvar Fernandez, B.;
693 van Dijk, M.E.A.; Tempelman, M.J.; Prakken, B.J.; de Jager, W. Effect of Anticoagulants
694 on 162 Circulating Immune Related Proteins in Healthy Subjects. *Cytokine* **2018**, *106*,
695 114–124, doi:10.1016/j.cyto.2017.10.021.
- 696 42. Skowronek, P.; Thielert, M.; Voytik, E.; Tanzer, M.C.; Hansen, F.M.; Willems, S.; Karayel,
697 O.; Brunner, A.-D.; Meier, F.; Mann, M. Rapid and In-Depth Coverage of the (Phospho-
698)Proteome With Deep Libraries and Optimal Window Design for Dia-PASEF. *Mol Cell*
699 *Proteomics* **2022**, *21*, 100279, doi:10.1016/j.mcpro.2022.100279.
- 700 43. Demichev, V.; Messner, C.B.; Vernardis, S.I.; Lilley, K.S.; Ralser, M. DIA-NN: Neural
701 Networks and Interference Correction Enable Deep Proteome Coverage in High
702 Throughput. *Nat Methods* **2020**, *17*, 41–44, doi:10.1038/s41592-019-0638-x.
- 703 44. Bizzarri, D.; Reinders, M.J.T.; Beekman, M.; Slagboom, P.E.; van den Akker, E.B. MiMIR:
704 R-Shiny Application to Infer Risk Factors and Endpoints from Nightingale Health’s 1H-
705 NMR Metabolomics Data. *Bioinformatics* **2022**, *38*, 3847–3849,
706 doi:10.1093/bioinformatics/btac388.
- 707 45. Chen, E.Y.; Tan, C.M.; Kou, Y.; Duan, Q.; Wang, Z.; Meirelles, G.V.; Clark, N.R.; Ma’ayan, A.
708 Enrichr: Interactive and Collaborative HTML5 Gene List Enrichment Analysis Tool. *BMC*
709 *Bioinformatics* **2013**, *14*, 128, doi:10.1186/1471-2105-14-128.
- 710 46. Sayols, S. Rvgo: A Bioconductor Package for Interpreting Lists of Gene Ontology Terms.
711 *MicroPubl Biol* **2023**, *10.17912/micropub.biology.000811*,
712 doi:10.17912/micropub.biology.000811.
713
714
715

716 **Figures Legends**

717 **Figure 1: Study description.** A) Flowchart detailing the inclusion criteria for samples within
718 each study population. B) Contrast in MetaboHealth, lymphocyte percentage, age and BMI
719 within each cohort.

720
721 **Figure 2: Increase GDF15, IL6, and MIG associate with MetaboHealth levels.** A) Differential
722 detectability between cases (top) and controls (bottom) for the Luminex cytokine measures,
723 with detected values in blue and undetected in grey. The heatmap on the bottom details the
724 adjusted p-value of the Fisher test evaluating the significances of the differential
725 detectability. C) Volcano-plot pertaining the univariate associations between the cytokines'
726 levels and the participants' case/control status corrected for sex, and age. In red the
727 positively associated cytokines, in grey the ones not significant. D) Heatmap depicting the
728 correlations between each cytokines with the components of the MetaboHealth score.

729
730 **Figure 3: Quantitative plasma proteomics reveals proteins that associate with**
731 **MetaboHealth scores in RS and LLS-PAROFFS cohorts.** A) Volcano plot depicting associations
732 of proteins with MetaboHealth scores (corrected for sex, and age). In blue the negatively
733 and in red the positively associated plasma proteins are depicted. Grouped significantly
734 enriched Gene Ontology Biological Processes are shown for B) the negatively and C)
735 positively associated plasma proteins. D) and E) depict the enriched KEGG pathways for the
736 plasma proteins respectively negatively and positively associated with the MetaboHealth
737 score.

738
739 **Figure 4: Plasma proteins associated with extreme MetaboHealth scores validated in the**
740 **NTR dataset.** A) Profile depicting the values of the most significantly associated proteins
741 ($|\text{estimate}| > 1$) and cytokines (y-axis) in all samples (x-axis), clearly separating the cases and
742 controls in all 3 datasets. The annotation on the top show the phenotypic characteristics of
743 all individuals. The annotation on the left shows the associations' estimate, and $\log_{10}(\text{FDR})$
744 observed in RS and LLS, and the platform for each feature (Mass Spectrometry based Plasma
745 Proteomics or Luminex). B) Beta-beta plot comparing the linear models in the extremes of
746 RS and LLS_PAROFFS on the x-axis and the linear mixed models in the NTR on the y-axis. Each
747 dots corresponds to a feature, and it's colored based on significance. The labels are shown
748 only when the features are consistently significant in the 2 analyses.

749
750

751 **Supplementary Figures legends**

752

753 **Figure S1: Quality control of the cytokines in LLS-PAROFFS and RS.** A) Percentage
754 of undetected values for each cytokine (x-axis) divided per cohort (y-axis). Differential
755 detectability analysis performed separately for B) LLS-PAROFFS and C) RS. Cytokines
756 distributions C) before and D) after the pre-processing steps (log transform and z-scaling).

757

758 **Figure S2: Sensitivity analyses and Meta-analyses of the cytokines' associations with**
759 **MetaboHealth extremes:** A- D) Volcano-plot of the univariate linear associations between
760 the cytokines and the case/control status of the participants systematically corrected by
761 increasing covariates. In grey the not significant cytokines and red the positively significant

762 ones. E) Intercorrelations of all the cytokines. F) Forest plots of the univariate linear
763 associations divided in RS (green), LLS-PAROFFS (yellow), and Meta-analyses (red).

764

765 **Figure S3: Quality control of the proteomics dataset in RS and LLS-PAROFFS:** A)
766 Percentage of missingness in the highly missing features divided per cohort. B) Differential
767 detectability between cases (top) and controls (bottom) for the proteins showing significant
768 difference. The heatmap on the bottom details the adjusted p-value of the Fisher test
769 evaluating the significance of the differential detectability. 9 randomly selected plasma
770 proteins distributions C) before and D) after the pre-processing steps (log transform and z-
771 scaling).

772

773 **Figure S4: Sensitivity analyses and Meta-analyses of the plasma proteins with the**
774 **MetaboHealth extremes in RS and LLS-PAROFFS:** A- D) Volcano-plot of the univariate
775 linear associations between the cytokines and the case/control status of the participants
776 systematically corrected by increasing covariates. In grey the not significant cytokines, in
777 blue the negatively and red the positively significant plasma proteins. Upset plot detailing the
778 amount of significantly D) negatively and E) positively associated features after correcting
779 for covariates.

780

781 **Figure S5: Meta-analyses of the associations between the proteomics features and the**
782 **MetaboHealth extremes:** Forest-plot of the meta-analysis for the significantly A) Negatively
783 and B) positively associated features.

784

785 **Figure S6: Correlations of the significantly associated proteomics:** Heatmaps of the
786 correlations of the proteomics features with A) MetaboHealth and its components, and B)
787 with the proteomics features themselves.

788

789 **Figure S7: Functional Enrichments of the proteomics datasets:** Bar-plots displaying the
790 log₁₀pvalues of the significant enrichments performed for all 320 features in the platform in
791 A) GO Biological Processes pathways, and B) KEGG pathways. GO Biological Processes
792 significantly enriched in the C) negatively and D) positively associated proteomics features.
793 Reactome pathways significantly enriched in the E) negatively and F) positively associated
794 proteomics features.

795

796 **Figure S8: Covid related proteins.** Plots displaying the case/control (red/blue) differences
797 in RS and LLS-PAROFFs for the proteins previously associated to covid infection by Völmy et
798 al.

799

800 **Figure S9: Pre-processing in NTR.** A) Percentage of undetected values per cytokines (y-
801 axis) per sample (x-axis). B) Percentage of undetected values per proteomics feature (y-axis)
802 in each sample (x-axis). C) Differential detectability of the cytokines in NTR.

803

804

805 **Figure S10: Associations in NTR.** Volcano plot of the univariate linear mixed models
806 comparing the case/control status with A) cytokines and B) proteomics features corrected
807 for age, and sex. Upset plots of the significantly C) negative and D) positive proteomics
808 markers.

809

810 **Figure S11: Complete Heatmap profiles of the significant proteins.** Profile depicting the
811 values of the significantly associated proteins (FDR<0.05) and cytokines (y-axis) in all
812 samples (x-axis), clearly separating the cases and controls in all 3 datasets. The annotations
813 on the top show the phenotypic characteristics of all individuals. The annotation on the left
814 shows the associations' estimate, and $\log_{10}(\text{FDR})$ observed in RS and LLS, and the platform
815 for each feature (Mass Spectrometry or Luminex).
816

Figure 1: MetaboHealth-driven selection and main phenotypic differences

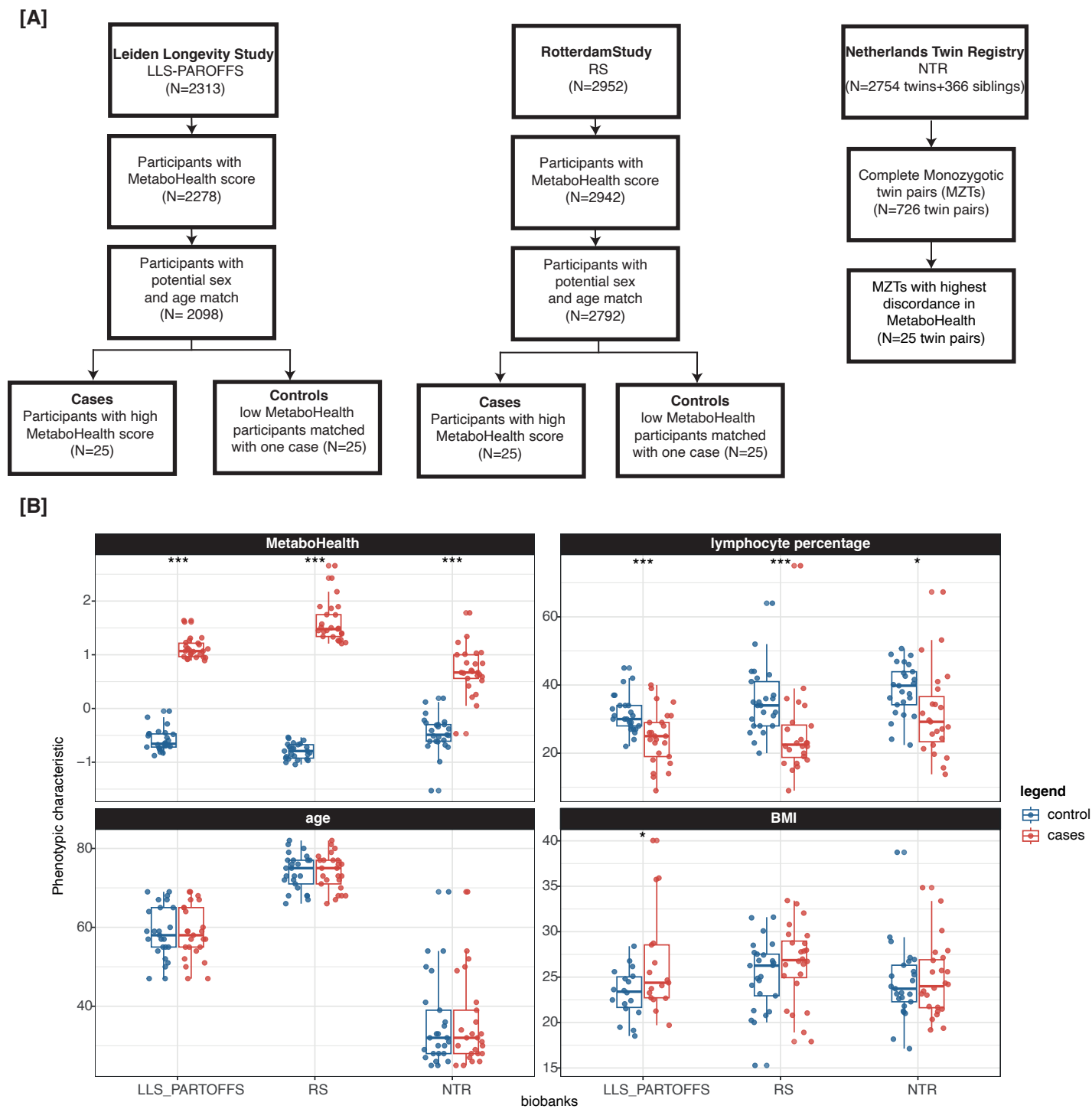


Figure 2: Increased GDF15, IL6 and MIG associate with higher MetaboHealth levels

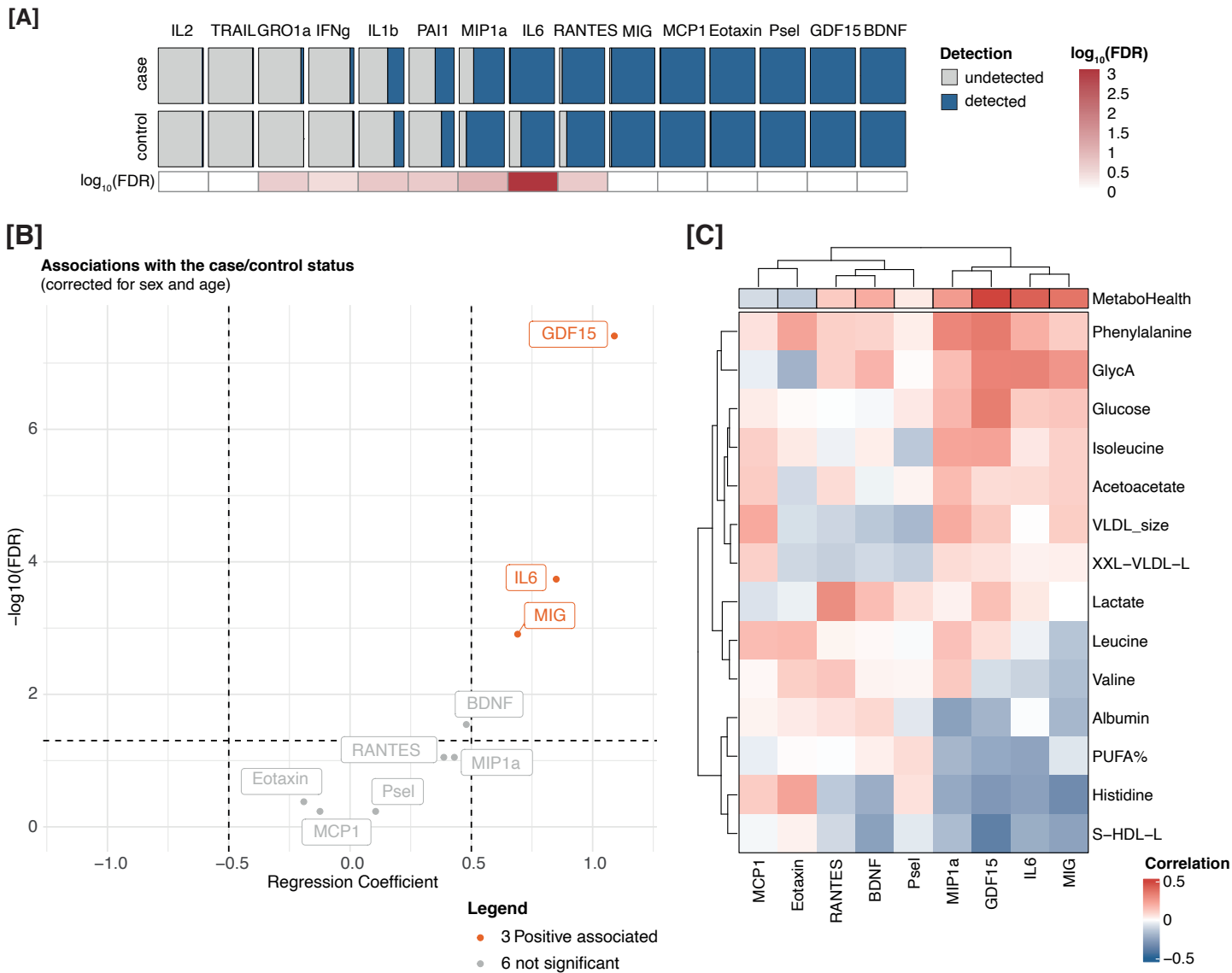
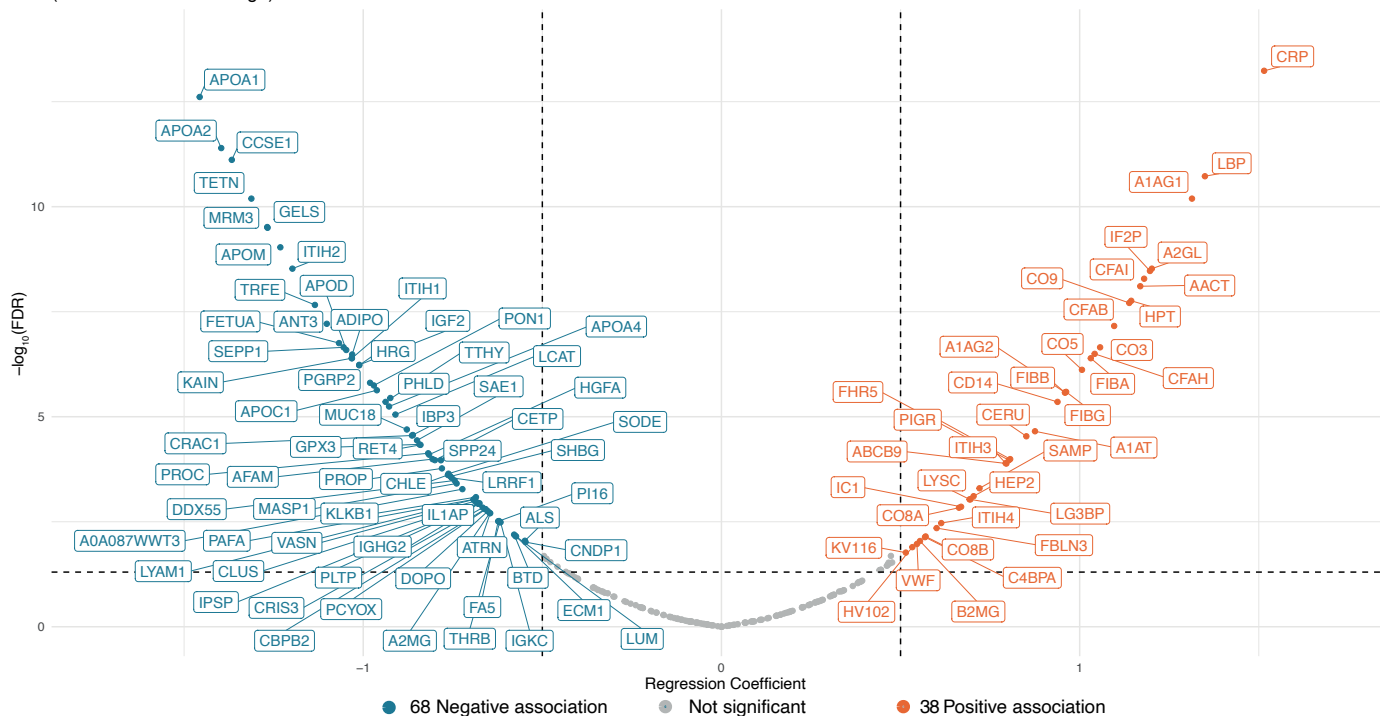
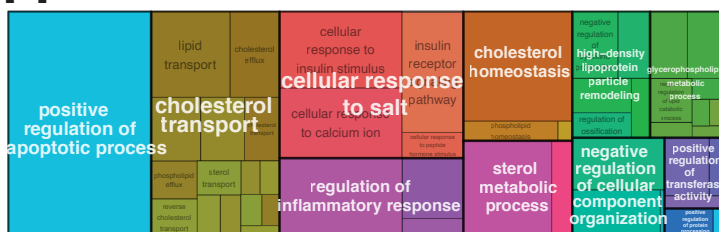


Figure 3: 68 negatively and 38 positively associated serum proteins

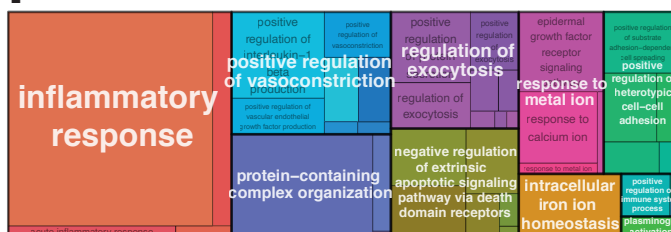
[A] Associations case/control
(corrected for sex and age)



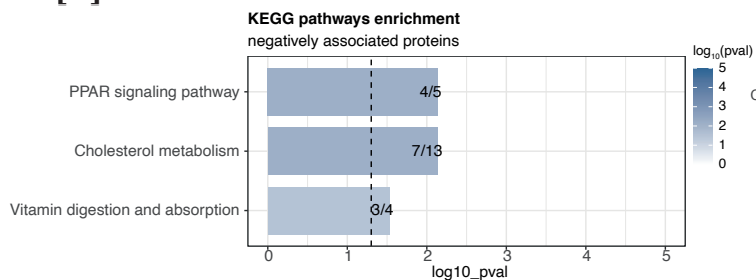
[B]



[C]



[D]



[E]

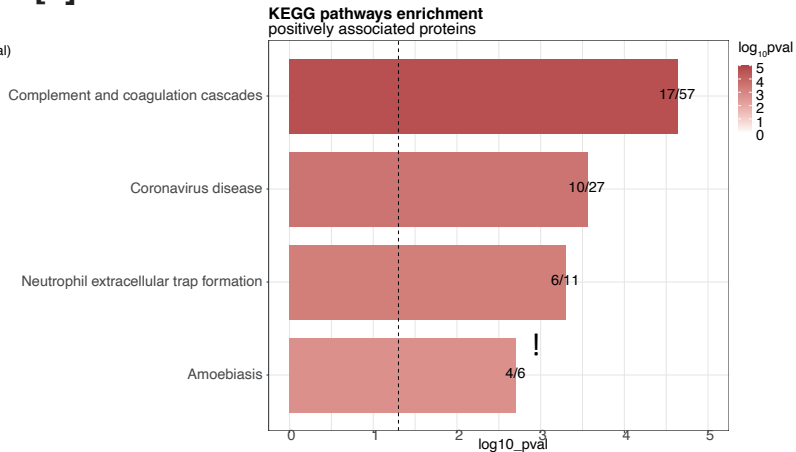


Figure 4: Proteomics associations to MetaboHealth in the monozygotic twins of NTR

